International Journal of Automotive Technology, Vol. 23, No. 3, pp. 829–840 (2022)
DOI 10.1007/s12239–022–0074–2

pISSN 1229–9138/ eISSN 1976–3832

PERSONALIZED SPEED PLANNING ALGORITHM USING A STATISTICAL DRIVER MODEL IN CAR-FOLLOWING SITUATIONS

Seung Eon Baek[1)], Hak Su Kim[2)] and Manbae Han[3)*]

[1)]Department of Automotive Engineering, Hanyang University, Seoul 04763, Korea
[2)]Strategic Planning Department, Control Works Inc., 13 Eonju-ro 81-gil, Gangnam-gu, Seoul 06222, Korea
[3)]Department of Mechanical and Automotive Engineering, Keimyung University, Daegu 42601, Korea

(Received 20 May 2021; Revised 23 December 2021; Accepted 10 January 2022)

ABSTRACT–Advanced driving assistance systems (ADAS) such as adaptive cruise control (ACC), traffic jam assistance, and collision warning have been developed to enhance driving comfort and reduce the driving burden in car-following situations. Although these systems provide automated driving to ensure safety, those do not harmonize the intentions of the driver by reflecting individual drivers' characteristics. To ensure that system reflects driver intention, we propose a personalized longitudinal speed planning algorithm in car-following situations, which system mimics personal driving styles. Individual driving styles were characterized by designing a pedal behavior prediction model and time headway distribution prediction model. The pedal behavior prediction model is an ensemble tree-based classifier that estimates the driver's current driving state, i.e., accelerating, cruising, or braking. Then, the driver-specific time headway distribution is estimated based on the polynomial model. These two prediction models were applied to the existing sampling-based speed planning algorithm and implemented with MATLAB/Simulink. The entire speed planning algorithm was simulated using vehicle simulation software. The simulation results showed that the actual driver's driving style was successfully reproduced.

KEY WORDS : Personalized speed planning, Prediction and cost function-based algorithm, Car-following situation, Time headway distribution, Driver model, Ensembles of trees, Kullback-Leibler divergence

NOMENCLATURE

d	: distance, m
v	: velocity, km/h
a	: acceleration, m/s^2
t	: time, s
μ_{THW}	: mean of time headway distribution, s
σ_{THW}	: standard deviation of time headway distribution, s
N	: number of iteration
$\hat{y}$	: predicted value
y	: actual value
C	: cost function
ω	: weight of each cost function
F	: cumulative probability density function
P	: probability density function
kd	: ACC control algorithm gain related to distance
kv	: ACC control algorithm gain related to velocity

subscripts

rel	: relative
ego	: ego-vehicle
preced	: preceding vehicle
max	: maximum value
min	: minimum value
i	: iteration number
pre	: prediction
cur	: current
des	: desired
cd	: control delay
vd	: vehicle delay
tot	: total
comf	: comfort
ref	: reference

*Corresponding author. e-mail: mbhan2002@kmu.ac.kr

1. INTRODUCTION

For the past several decades, advanced driving assistance system (ADAS) and autonomous vehicle (AV) technologies have evolved rapidly (Kuwata *et al.*, 2009). Currently commercially available autonomous driving systems such as adaptive cruise control (ACC), stop & go (S&G), and collision warning/collision avoidance (CW/CA) have been known to improve passenger comfort in car-following situations (Bishop, 2000). They have also contributed to reductions of driving burden and traffic accidents. However, these techniques have exposed a limitation in reflecting general driving behaviors rather than individual driving

characteristics. Therefore, these systems cause disharmony with drivers and, thus, result in poor system acceptance by drivers (Joshi *et al.*, 2009).

To alleviate this inconvenience, many automotive manufacturers provide several presets, e.g. cruising speed and time head way (THW); however, it remains difficult for a few presets in an ACC system to allow system to mimic individual driving styles (Reagan *et al*., 2017). Due to the wide variety of preferences of individual drivers and diverse personal experience and background according to age, gender, country, education, and income level, the design of a personalized autonomous driving system that can reflect individual driving styles has been treated as a challenging task (Moon and Yi, 2008; Lin *et al.*, 2014; Rosenfeld *et al.*, 2015; Martinez *et al.*, 2017; Zhu *et al.*, 2019).

Many studies for the design of personalized autonomous driving systems have been conducted by modeling human driving styles for personalized autonomous driving systems can be classified into group-based, deterministic, and stochastic approaches.

The group-based driver model classifies drivers into several groups based on their driving styles, such as 'aggressive', 'normal', and 'cautious'. Then, the mode-switching control was achieved using a driver model (Rosenfeld *et al.*, 2015; de Gelder *et al.*, 2016; Zhu *et al.*, 2019). Rosenfeld *et al*. (2015) classified drivers into three groups through a large data set and, using a regression model and a decision tree, predicted the THW preferred by drivers in the group. Meanwhile, de Gelder *et al*. (2016) proposed a Support Vector Machine (SVM) based classifier that predicts the driver preferred. THW based on 20 test drivers' driving data. However, it is still challenging to design a personalized controller for every driver with this group-based driver model.

Deterministic driver models directly calculate control inputs such as speed, acceleration, and pedal operation based on individual driving style (Mikami *et al.*, 2010; Liebner *et al.*, 2012; Wang *et al.*, 2012; Butakov and Ioannou, 2015). Driver models composed of deterministic equations are more transparent and analytical than group-based driver models. However, it remains a challenge to model the stochastic behavior of real drivers because drivers exhibit stochastic reactions under the same driving conditions.

To reflect the stochastic characteristics of driving characteristics, some stochastic driver models have been proposed. For most of these driver models, the control inputs are calculated using the gaussian mixture model (GMM) or hidden markov model (HMM) trained with human-driven data (Miyajima *et al.*, 2007; Yang and Peng, 2010; Angkititrakul *et al*., 2011; Lefèvre *et al.*, 2015a; Wang *et al.*, 2017). These stochastic driver models have precisely explained the stochastic characteristics of drivers. However, with the exception of (Lefèvre *et al.*, 2015a), most of these studies have a limitation in that they do not perform experimental study and/or perform a simulation study using a vehicle model.

Aside from the above mentioned research using driver models, in recent years there have been many approaches to achieving personalized autonomous driving systems in various driving situations (Wei *et al*., 2010a; Gu *et al*., 2016; Lefèvre *et al*., 2015b; Driggs-Campbell *et al*., 2017; Li *et al.*, 2017; González *et al.*, 2018; He *et al.*, 2018). These studies were conducted based on a planning algorithm, which is considered a key technology of AV because it can present various performance indices and constraints better than is possible using conventional control algorithms. In several studies, a learning-from-demonstration technique was proposed to solve the inefficient cost-function tuning process that was performed in existing planning algorithm design (Gu *et al*., 2016; González *et al.*, 2018). The researchers used the novel inverse reinforcement learning (IRL) method to learn human driving styles in merging and overtaking situations. Moreover, He *et al*. (2018) proposed a sampling-based planning algorithm that generates a human-like trajectory by calculating the similarities between candidate trajectories and naturalistic driving data in lane-changing scenarios. This algorithm also involves the process of learning the selection policy based on naturalistic driving data to generate a human-like trajectory. Furthermore, Wei *et al*. (2010a) proposed a learning-based driver model that showed behavior similar to that of real drivers in car-following situations. Their model was designed by learning the cost-function of the prediction and cost function-based (PCB) algorithm based on human driving data. Most of these studies have focused on learning the cost functions or reward functions of the planning algorithm. However, although the planning algorithm designed in the above approach can mimic human driving styles, it has a limitation in that it is difficult to clearly describe the relationship between learned cost functions and human driving styles.

In this paper, we propose a statistical driver model that can mimic individual driving styles in car-following situations; we then apply it to the existing planning algorithm to achieve a personalized speed planning algorithm. To analyze the mechanism by which individual drivers determine pedal operation and control the vehicle in their preferred area in car-following situations, real driving data were acquired. We designed a driver model that predicts a driver's pedal behavior and his or her THW distribution in car-following situations because we reason that noticeable differences in THW distribution of individual drivers also strongly depend on the pedal behavior. To design this driver model, we used a bagged tree, a machine learning technique, and a polynomial regression. Then, the driver model was applied to the PCB algorithm. We implemented the proposed algorithm in MATLAB/Simulink and verified the algorithm using the commercial vehicle simulation software IPG CarMaker. The simulation results show that the proposed planning algorithm can reflect the driving styles of individual drivers. The remainder of this paper is structured

as follows. Data acquisition is described in Section 2. The statistical driver model is elaborated in Section 3. Section 4 contains an explanation of the personalized speed planning algorithm using the statistical driver model, which is followed by a discussion of the simulation results in Section 5. Finally, the conclusions of this study are presented in Section 6.

2. DATA ACQUISITION

2.1. Data Acquisition Environment

To perceive significant driver features for design of the driver model, driving data were acquired using an electric vehicle, a Hyundai KONA, equipped with various in-vehicle sensors and radar with a 150 m maximum range. Figure 1 shows the overall structure of the in-vehicle data flow. On-Board Diagnostics II (OBD II) was connected to the arbitrator using an Infineon TC237 through a CAN protocol. The measured data were logged using Vector VN1640. The real-time acquisition was synchronized and recorded at 100 Hz.

A two-lane straight urban road in Incheon, Korea, was selected as the driving environment, as shown in Figure 2. The 2.0 km route represented by the yellow line in Figure 2 is the actual test route. Data acquisition experiments were conducted with three drivers in car-following situations. A total of 36 km of driving data were accumulated from three round trips by three drivers who possessed different styles of driving.

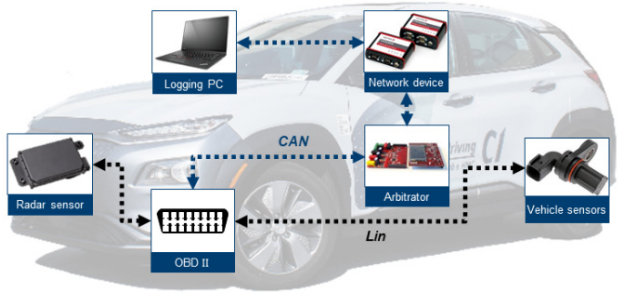

Figure 1. Schematic diagram of in-vehicle data flow.

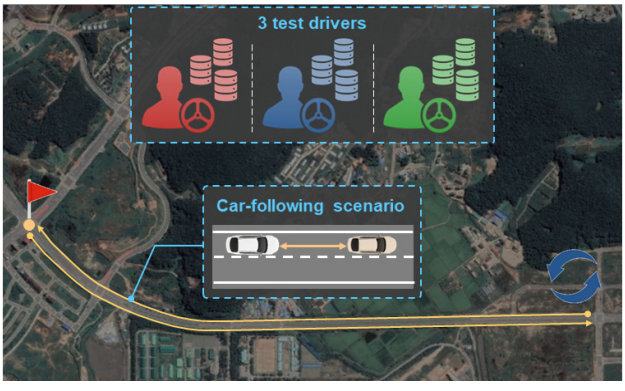

Figure 2. Driving environment.

2.2. Driving Data Analysis

Statistical analysis has been used in several studies to compare the means and standard deviations of driver features to distinguish driving styles of individual drivers in car-following situations (Moon and Yi, 2008; de Gelder *et al.*, 2016; Zhu *et al.*, 2019). Driver features in car-following situations are related to the ego-vehicle and the behavior of the preceding vehicle. Driver features related to the ego-vehicle include ego-vehicle velocity, acceleration, and jerk, i.e. a derivative of acceleration. Related to the behavior of the preceding vehicle is the relative velocity, a relative distance measured directly, THW, and Time to Collision at i^{th} time instant (TTCi). THW and TTCi, especially, have been considered crucial parameters to represent driver features, as elaborated in related works (Moon and Yi, 2008; Wang *et al.*, 2012; Lefèvre *et al.*, 2015c; Rosenfeld *et al.*, 2015; de Gelder *et al.*, 2016). Distributions of THW and TTCi distinguish individual drivers in car-following situations (Ohno, 2001; Yang and Peng, 2010; Rosenfeld *et al.*, 2015; Loulizi *et al.*, 2019; Zhu *et al.*, 2019). They are defined as in Equations (1) and (2), respectively:

$$\text{THW} = \frac{d_{rel}}{v_{ego}} \tag{1}$$

$$\text{TTCi} = \frac{d_{rel}}{v_{rel}} \tag{2}$$

where, d_{rel} the relative distance between the preceding vehicle and the ego-vehicle, v_{rel} is the relative velocity, and v_{ego} is the velocity of the ego-vehicle.

3. STATISTICAL DRIVER MODEL

The THW distribution of an individual driver is well known as an important feature of the driver model. We reason that noticeable differences in THW distribution of individual drivers also strongly depend on the pedal behavior (stepping on and off the accelerator pedal or brake pedal). Therefore, we propose a statistical driver model that combines a pedal behavior prediction model and THW distribution prediction model. The pedal behavior prediction model predicts which pedal operation the driver will perform based on the current vehicle state. The driving section, which is the output of the model, is defined by the driver's pedal behavior and is classified into the accelerating section (accelerator pedal), the cruising section (no pedal), and the braking section (brake pedal). Moreover, the THW distribution prediction model predicts the THW distribution for the near future based on initial driver features when driving section changes (accelerating, braking section).

3.1. Reasoning Why Pedal Behavior Prediction Model is Included in Driver Model

Based on the analysis of the driving data, individual drivers exhibit different pedal behaviors and, thus, different driving behaviors, which are confirmed by comparing the THW distribution results. Figures 3 and 4 show the THW distributions of individual drivers.

In Figure 3, the means and the standard deviations of the THW distributions can be seen to vary from driver to driver, indicating that the driving style of the individual drivers differs in car-following situations. Figure 4 presents differences in THW distributions according to pedal behavior of individual drivers. To analyze the causes of differences in driving style between individual drivers when accelerator or brake pedal is stepped on, we compared the driving conditions during which the drivers began to step on each pedal. Figure 5 shows scatter plots of the different conditions (velocity, relative velocity, THW, TTCi) when individual drivers initiate stepping on the accelerator pedal. In this figure, the red, blue, and green dots show the driving data for $Driver_1$, $Driver_2$, and $Driver_3$, respectively. For example, the second figure in first row shows the condition of time headway and velocity when three drivers initiate stepping the accelerator pedal. The $Driver_1$ steps on the pedal in the condition of faster velocity and lower time headway than $Driver_3$. It means that the $Driver_1$ tends to keep the distance from the preceding vehicle narrower at a faster speed than $Driver_3$. In the same manner, the driver's characteristics can be expressed by the difference in the distribution shown in the nine scattered plots. All subplots show that individual drivers begin stepping on the accelerator pedal under their own preferred driving conditions. Therefore, we defined the initial driver feature at which the driver steps on the accelerator or brake pedal, which is a significant factor distinguishing the driving styles of individual drivers. Hence, as shown in Figure 6, the statistical driver model is designed to mimic human driving style by combining the pedal behavior prediction model and the THW distribution prediction model.

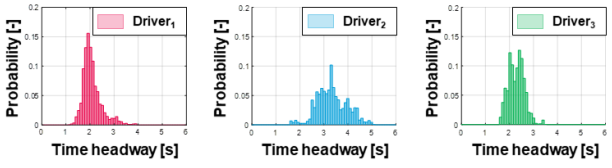

Figure 3. THW distribution of the individual drivers.

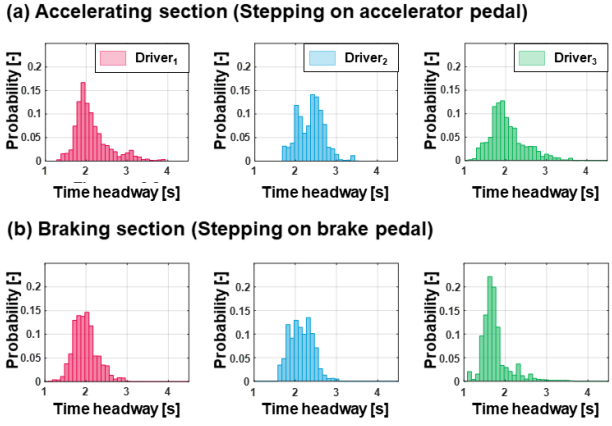

Figure 4. THW distributions of the individual drivers according to pedal behavior.

3.2. Pedal Behavior Prediction Model

The pedal behavior prediction model predicts which pedals driver will press at the current vehicle state. Due to the high variance of pedal behaviors of individual drivers, a bagged

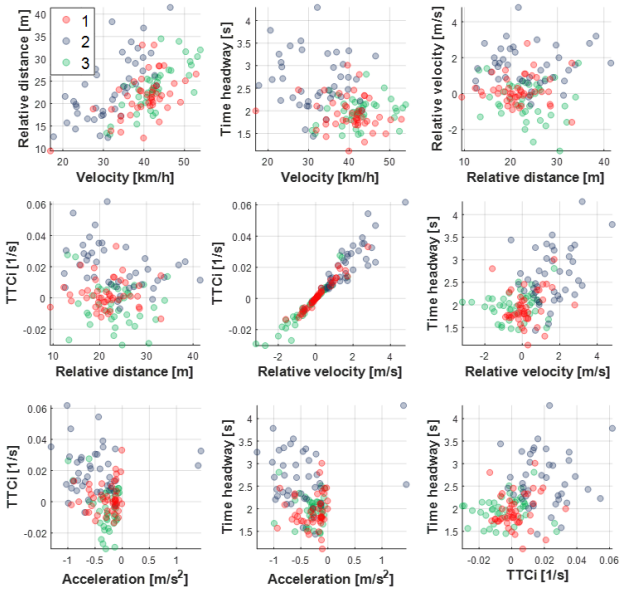

Figure 5. Initial driver features when the driver steps on the accelerator pedal.

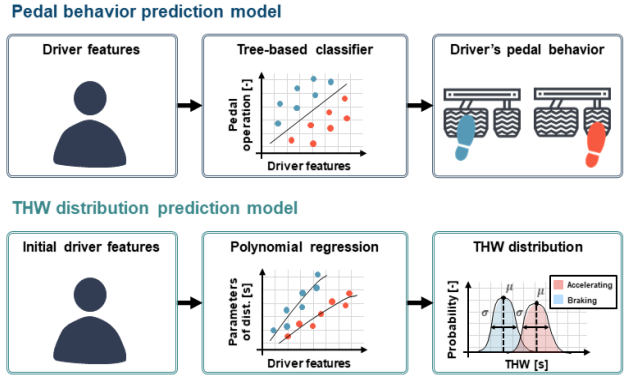

Figure 6. Structure of the statistical driver model.

tree based-classifier with high classification performance for low dimensional data sets was chosen to design the pedal behavior prediction model. A bagged tree, known as the 'ensembles of trees method', is a suitable method to solve the high-variance problem occurring when using a single tree based-classifier (Caruana and Niculescu-Mizil, 2006; Lou *et al*., 2012). To reduce the variance, this method uses some of the data to train numerous single trees and averages the classification results of these single trees.

The proposed pedal behavior prediction model was trained using the supervised machine learning toolbox in MATLAB based on the acquired driving data. The inputs to the model, which predict these driving sections, are as follows: v_{ego}, ego vehicle's acceleration (a_{ego}), d_{rel}, v_{rel}, THW, TTCi. The outputs of the model are three driving sections: accelerating section (accelerator pedal), braking section (brake pedal), cruising section (no pedal). The inputs and outputs of the model are summarized in Table 1.

To train the proposed model, more than 5000 data samples were used for each driver. 70 % of the data were chosen as the training set and the other 30 % were chosen as the test set. Moreover, to enhance the model performance, we performed parameter optimization of the bagged tree-based prediction model using Bayesian optimization, which has been utilized as a method for optimizing hyperparameters in various machine learning techniques. In this step, the objective function is defined as a function that outputs the loss of the model according to the parameters of the bagged tree. Bayesian optimization was then performed, which consists of estimating the defined objective function through the Gaussian Process (GP) model trained using certain parameters-loss pairs and searching the optimal parameters by learning the GP model through the acquisition function. In this paper, the optimal parameters of the bagg, such as the number of single trees and minimum leaf size, are different for individual drivers. The optimal parameters are reported in Table 2.

To analyze the results of the pedal behavior prediction model for individual drivers in detail, confusion matrices are plotted and shown in Figure 7. In this figure, the diagonal cells show the number and percentage of correct predictions of cruising, braking, and accelerating sections.

Taking the confusion matrix of driver1 as an example, during the whole test set, 45.6 % of the data predicted accelerating sections correctly, 40.9 % of data predicted braking sections correctly, and 12.4 % of data predicted cruising sections correctly. The non-diagonal cells show where the wrong predictions occurred and the rightmost column in gray shows the accuracy of each prediction result. For example, in the third column of the first row, even though the actual driving sections were cruising sections, the data incorrectly predicted these to be accelerating sections as three times. As a result, the first cell in the rightmost column shows that 99.6 % of the results were correctly predicted as accelerating section and 0.4 % of the results were wrongly predicted. The bottom row in gray shows the prediction accuracy for each actual driving section. For example, the first cell in the bottom row shows that 99.5 % of the results correctly predicted the acceleration section and 0.5 % of the results incorrectly predicted the acceleration section as the cruising section. The cell in the lower right corner shows the overall accuracy of 98.9 % of the model's predictions of driving section of driver1. Finally, the yellow dashed cells show that the proposed prediction model does not confuse the accelerating and braking sections. These results are important because the driving styles of individual drivers are significantly different in acceleration and braking sections; results also show that the proposed prediction model for all drivers meets the previously enumerated requirements.

Table 1. Inputs and outputs of the prediction model.

	Variable
Input	Ego-vehicle velocity
	Acceleration
	Relative distance
	Relative velocity
	THW
	TTCi
Output	Accelerating section (accelerator pedal)
	Braking section (brake pedal)
	Cruising section (no pedal)

3.3. Time Headway Distribution Prediction Model

From the analysis of the car-following situation, it was realized that drivers tend to maintain different THW values for each driving section by stepping on different pedals. To reflect this in the speed planning algorithm, a THW distribution prediction model that predicts the THW distribution for each driving section was designed. As shown in Figure 8, for parametric design purposes, the THW distribution for each driver is assumed to be Gaussian. Moreover, the parameters of the distribution (the maximum THW, the minimum THW, the mean and the standard deviation) were modeled using the second-order polynomial regression method based on the initial driver features; their functional equations are described, respectively, below:

Table 2. Parameters of the bagged tree.

	$Driver_1$	$Driver_2$	$Driver_3$
Number of single trees	371	493	495
Minimum leaf size	1	2	1

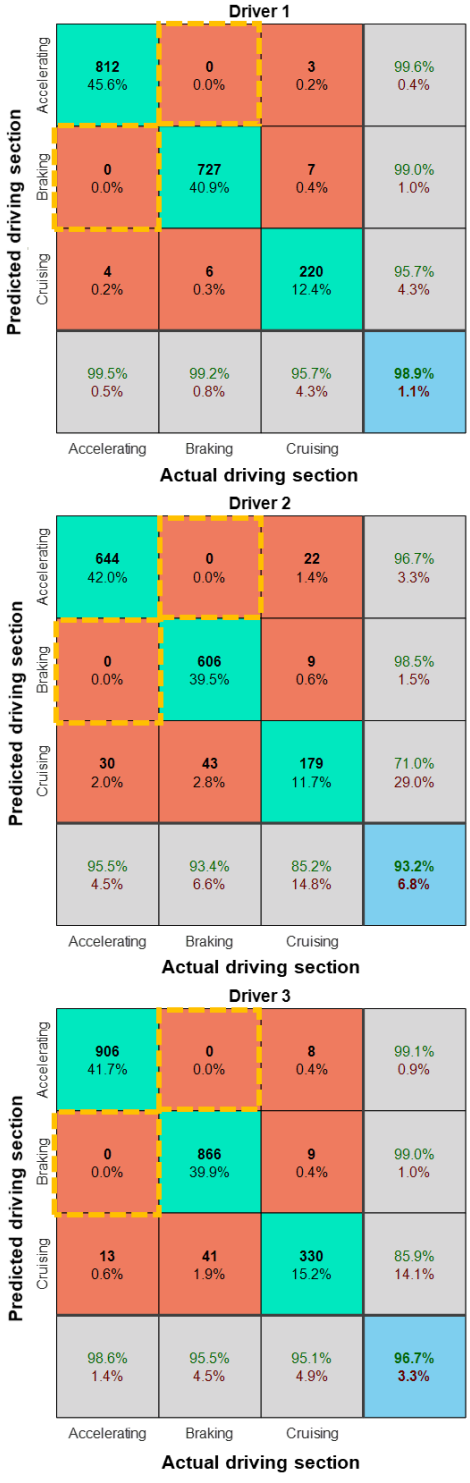

Figure 7. Confusion matrices for prediction results.

$$\mathrm{THW}_{max} = f\left(v_{rel}, \mathrm{TTCi}, \mathrm{THW}, v_{ego}\right) \quad (3)$$

$$\mathrm{THW}_{min} = f\left(v_{rel}, \mathrm{TTCi}, \mathrm{THW}, v_{ego}\right) \quad (4)$$

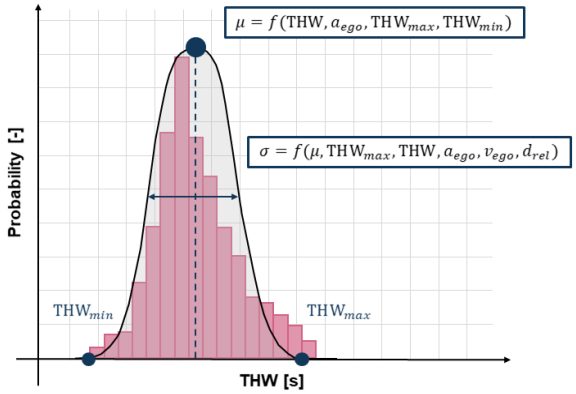

Figure 8. Parameters of the THW distribution assumed as Gaussian.

$$\mu_{\mathrm{THW}} = f\left(\mathrm{THW}_{min}, \mathrm{THW}_{max}, \mathrm{THW}, a_{ego}\right) \quad (5)$$

$$\sigma_{\mathrm{THW}} = f\left(\mu_{\mathrm{THW}}, \mathrm{THW}_{max}, v_{ego}, d_{rel}, a_{ego}\right) \quad (6)$$

where, μ_{THW} means the mean of THW distribution and σ_{THW} means the standard deviation of THW distribution. The design variables of the proposed distribution prediction model are reported in Table 3.

Though the prediction of μ_{THW} and σ_{THW} by using the driver features as independent variables is challenging, it can be simplified by estimating THW_{max} and THW_{min}. The proposed prediction model was designed to predict the THW distribution in the driving section through the initial driver features at the moment the predicted pedal behavior changes. The accuracy of the proposed prediction model was verified through a Quantile-Quantile (Q-Q) plot (Figure 9) and using evaluation metrics, such as the coefficient of determination R^2, and the root-mean-squared of error (RMSE), which are respectively given as

$$\bar{y} = \frac{1}{N}\sum_{i=1}^{N} y_i \quad (7)$$

$$\mathrm{R}^2 = 1 - \frac{\sum_{i=1}^{N}(y_i - \hat{y}_i)^2}{\sum_{i=1}^{N}(y_i - \bar{y})^2} \quad (8)$$

$$\mathrm{RMSE} = \sqrt{\frac{\sum_{i=1}^{N}(y_i - \hat{y}_i)^2}{N}} \quad (9)$$

where, $\bar{y}$ denotes the average of the actual values y_i, and $\hat{y}_i$ denotes the predicted values. R^2 is an index that can measure the accuracy of the model. Figures 9 (a) and 9 (b) show the regression performance of the mean and standard deviation, respectively, of the THW distribution for the accelerating section. The modeling results show that the prediction accuracy is significant, although somewhat different for each driver, as expected.

Table 3. Initial driver features correlated with the parameters of THW distribution.

Parameter	Correlated initial driver features
THW_{max}	Relative velocity, TTCi, THW, velocity
THW_{min}	Relative velocity, TTCi, THW, velocity
μ_{THW}	THW_{max}, THW_{min}, THW, acceleration
σ_{THW}	μ_{THW}, THW_{max}, velocity, relative distance, acceleration

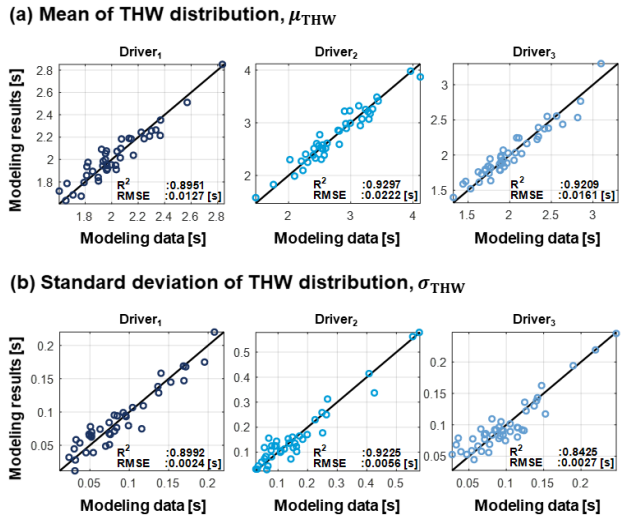

Figure 9. Results of the THW distribution prediction model for accelerating sections (a) μ_{THW}, (b) σ_{THW}.

4. PERSONALIZED SPEED PLANNING ALGORITHM

4.1. Overall Structure

The personalized speed planning algorithm generates a personalized speed trajectory by utilizing the predicted THW distribution, which is predicted by the statistical driver model via receiving the driver features as inputs, as shown in Figure 10. The PCB algorithm utilizes the THW distribution to generate the speed trajectory. The process of the PCB algorithm is as follows: candidate THW strategy generation, speed trajectory prediction, and cost function-based strategy evaluation, as shown in Figure 11. In Figure 11, t_{pre} is the prediction time, which is the length of the speed trajectory generated through the PCB algorithm.

4.2. Candidate THW Strategy Generation

In the candidate THW strategy generation step, a certain number of strategies are generated by the predicted THW distribution from the statistical driver model, while the conventional PCB algorithm generates THW distribution using random uniform sampling regardless of the current driving section. Figure 12 shows the process of generating THW strategies, which includes random sampling and profiling. As shown in the figure, this step generates driver-preferred THW strategies, which is a crucial difference from the previous PCB algorithm. Moreover, the following steps convert each driver preferred THW strategy into a personalized speed trajectory.

4.3. Speed Trajectory Prediction

In the speed trajectory prediction step, the generated THW strategies are forward-simulated in a prediction engine capable of simulating car-following from a microscopic perspective to predict the speed trajectories corresponding to each THW strategy (Wei and Dolan, 2009; Wei *et al.*, 2010b; Wei *et al.*, 2014). The generated THW strategies are converted into speed trajectories in the prediction engine. As shown in Figure 13, the prediction engine receives the THW strategy as a control input of ego-vehicle's ACC algorithm, as described in Figure 14. Moreover, the preceding vehicle's speed assumed a Constant Velocity (CV) model. We denote the assumed velocity of the preceding vehicle as v_{preced}.

4.4. Cost Function-based Evaluation

In Figure 14, $d_{rel,des}$ is the desired relative distance, v_{ego} is the ego-vehicle velocity, kd and kv are parameters of the controller, v_{des} is the desired velocity, and a_{des} is the desired

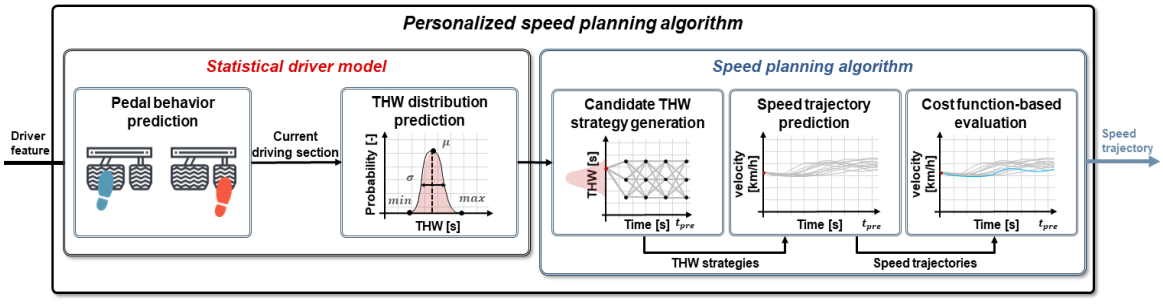

Figure 10. Overall structure of the personalized speed planning algorithm.

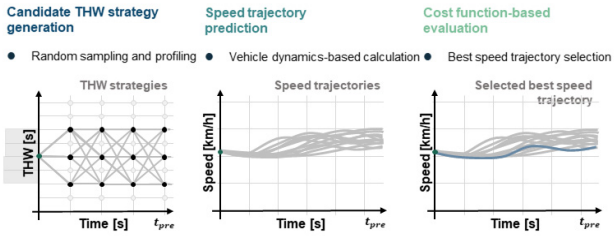

Figure 11. Conventional PCB algorithm process.

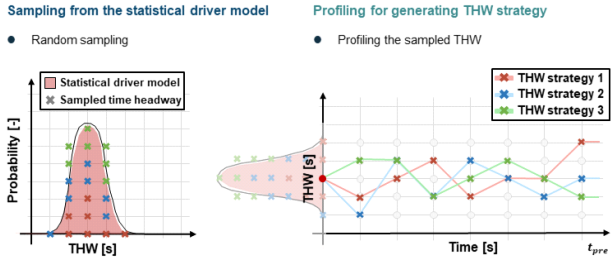

Figure 12. Candidate THW strategy generation step.

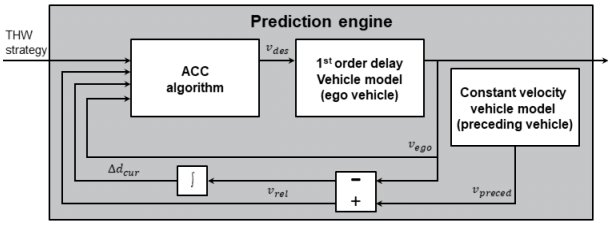

Figure 13. Diagram of the prediction engine.

ACC algorithm

1: **for** t = 1: t_{pre}

Calculation of desired velocity

2: $d_{rel,des}(t) = v_{ego}(t) * THW\ strategy(t)$

3: $d_{rel,des}(t) = \mathbf{max}(d_{rel,cur}(t), 5m)$

4: $a_{des}(t) = \left(d_{rel,cur}(t) - d_{rel,des}(t)\right) * kd + v_{rel}(t) * kv$

5: $v_{des}(t) = v_{ego}(t) + a_{des}(t) * t$

Calculation of velocity

7: $v_{ego}(t+1) = (1 - t_{cd})v_{ego}(t) + t_{cd} * v_{des}(t - t_{vd})$

where t_{cd} is control time delay and t_{vd} is vehicle delay

8: **end**

9: Return $\boldsymbol{v_{ego}}$

Figure 14. ACC algorithm in the prediction engine.

acceleration. The ACC algorithm first calculates the desired safety distance of the control target using the THW strategy at each step. Subsequently, ego-vehicle's speed trajectories, considering vehicle time delay t_{vd} and control time delay t_{cd}, are predicted corresponding to the generated THW strategies.

In the cost function-based evaluation step, the generated speed trajectories are evaluated with a pre-defined cost function:

$$C_{total} = \omega_{track}C_{track} + \omega_{comf}C_{comf} + \omega_{safe}C_{safe} \quad (10)$$

$$C_{track} = \sum_{t=1}^{t_{pre}} \left(\frac{d_{des}}{v_{ego}} - \frac{d_{cur}}{v_{ego}}\right)^2 \quad (11)$$

$$C_{comf} = \sum_{t=1}^{t_{pre}} \left(\omega_{acc} {v'_{ego}}^2 + \omega_{comf} {v''_{ego}}^2\right) \quad (12)$$

$$C_{safe} = \sum_{t=1}^{t_{pre}} f(d_{cur}, v_{ego}) \quad (13)$$

where the total cost includes tracking cost, comfort cost, and safety cost. The tracking cost C_{track} verifies the controllability of the candidate THW strategy. The comfort cost C_{comf} punishes fast acceleration and fast jerk as a squared sum of acceleration and jerk. Lastly, the safety cost C_{safe} penalizes candidate THW strategies that engage the ego-vehicle in dangerous situation such as approaching the preceding vehicle too quickly, as previously proposed in (Wei *et al.*, 2014).

After the evaluation, the personalized speed trajectory was selected. We then performed the simulation to verify whether or not the proposed planning algorithm reflects individual driver's driving styles.

5. SIMULATION RESULTS

5.1. Simulation Environment

To verify the proposed planning algorithm, a simulation environment including a test track, preceding vehicle and radar sensor was developed with commercial vehicle simulation software (IPG CarMaker); this setup provides the various sensor models required for ADAS and is a simulation software that can freely configure the shape of the test track and behavior of the surrounding vehicles. In addition, it has detailed fidelity at the vehicle powertrain level and has been used extensively in powertrain research (Shin *et al.*, 2019) and connected vehicles (Boudali *et al.*, 2020), as well as ADAS (Mitra *et al.*, 2018; Gao and Gordon, 2019; Ilić *et al.*, 2019; Kale *et al.*, 2019). The Hyundai KONA in IPG CarMaker was virtually modeled and used for data acquisition to extract reliable simulation results; Table 4 shows the specifications of the vehicle. Furthermore, to generate output from the proposed planning algorithm, a velocity tracking controller is required to control the vehicle in IPG CarMaker. Controller was designed with a hierarchical structure that has been widely adopted in the

longitudinal control of vehicles, including a higher-level controller as a model predictive control (MPC)-based controller that can systematically handle the constraints and nonlinearities of the vehicle system and a lower-level controller as a simple PID based controller (Gray *et al.*, 2013; Li *et al.*, 2017). Thus, the speed trajectory generated by the planning algorithm was used as the input to the higher-level controller, which then output the reference acceleration (a_{ref}) required to track the input of the inputted speed trajectory. Likewise, the lower-level controller outputs the normalized pedal position that follows a_{ref}.

To verify the proposed planning algorithm designed with MATLAB/Simulink, the proposed algorithm and IPG CarMaker were integrated through the CarMaker For SimuLink (CM4SL) library. Through this library, the control outputs of the velocity tracking controller, such as the accelerator and brake pedal positions, were connected to the internal variables of the virtual vehicle.

The entire simulation environment was constructed as shown in Figure 15. First, in MATLAB/Simulink, the proposed planning algorithm and velocity tracking controler were implemented and the normalized pedal positions were calculated. Next, the CM4SL library was used to convert the control output to the internal variables. Then, the ego-vehicle was controlled via inputting a pedal position in the IPG CarMaker. Finally, the internal variables including the ego-vehicle states and the preceding vehicle states were fed back into the proposed algorithm and velocity tracking controller.

To verify that the proposed planning algorithm can reflect actual drivers' driving styles, the vehicle in car-following situations was controlled with the proposed planning algorithm using the different driver models for the same preceding vehicle behavior that was acquired in the vehicle experiments (Figure 16).

5.2. Results Analysis

The simulation results of the proposed planning algorithm are presented in Figures 17 ~ 18 and Tables 5 ~ 6. In Figure 17, the driving results are plotted in the time domain. The yellow line shows the behavior of the preceding vehicle. The red, blue, and green lines show the driving data of the proposed planning algorithm using the different driver models ($Driver_1$ ~ $Driver_3$). The simulation results show that for the same preceding vehicle, only the ego-vehicle behavior differed according to the driver model used in the proposed algorithm. The results indicate that the proposed planning algorithm works well in car-following situations. Furthermore, these results show that even if the initial conditions such as Figure 17 (a) speed, Figure 17 (b) relative distance, and Figure 17 (c) THW are the same, the driving results of the proposed algorithm using different driver models will be different. In particular, the THW trajectories show that the proposed planning algorithm controls the vehicle while maintaining THW that actual drivers prefer.

Table 4. Specification of vehicle (Hyundai KONA).

Vehicle parameter	Value	Powertrain parameter	Value
Unloaded weight	1685 kg	Maximum torque (Motor)	395 Nm
Length	4180 mm	Maximum power (Motor)	150 kW
Width	1800 mm	Maximum rpm (Motor)	11000 rpm
Height	1570 mm	Inertia (Motor)	0.028 kg·m^2
Driving axle	Front driven	Capacity (Battery)	180 Ah 64 kWh
Tire specification	215/55 R	Idle voltage (Battery)	353 V
Tire radius	17 inch	Maximum power (Battery)	150 kW

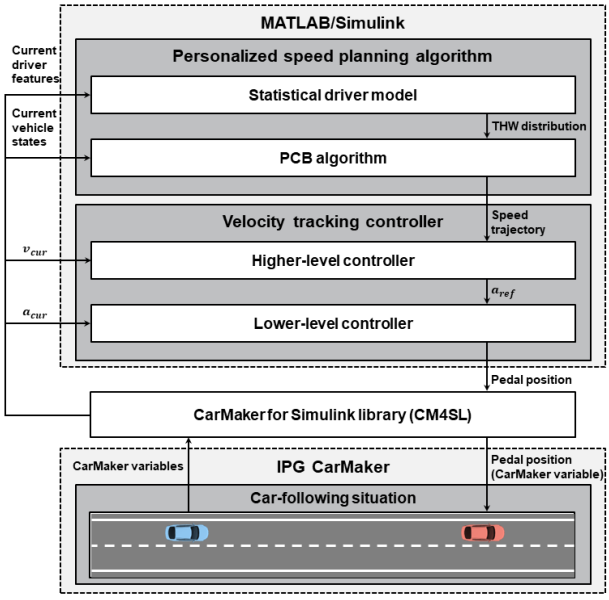

Figure 15. Simulation environment.

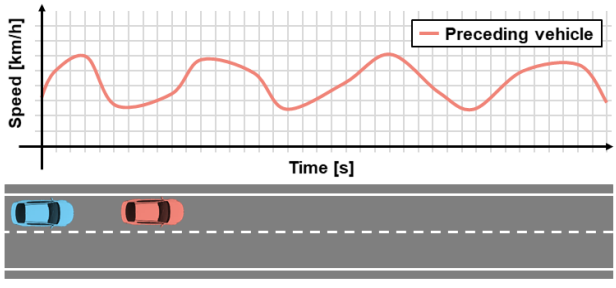

Figure 16. Simulation scenario.

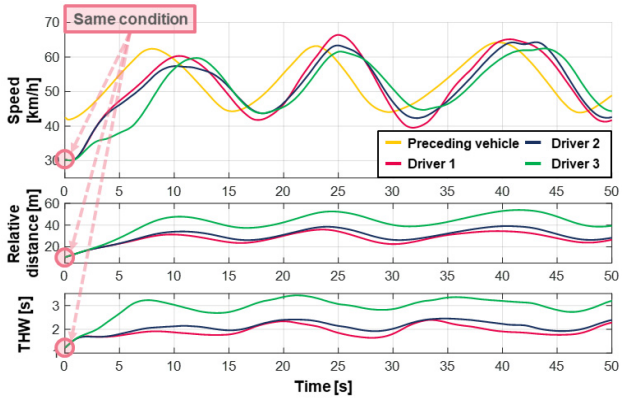

Figure 17. (a) Speed; (b) Relative distance; (c) THW simulation results in the time domain.

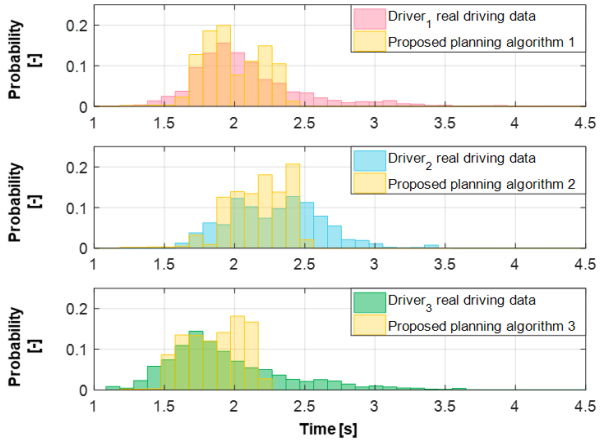

Figure 18. Comparison of the driving data for the real driver and the proposed algorithm.

Also, THW distributions of the simulated and real driving data were compared to verify that the outcomes of using the simulated driving data were similar to actual driver's driving styles. Figure 18 shows driving data of actual drivers and from the proposed planning algorithm. The yellow distributions show driving data for the proposed algorithm using different driver models, while the red, blue, and green distributions show the driving data of the real drivers. The K-S distance and the K-L divergence were used to objectively evaluate the similarity between driving style of the proposed planning algorithm and the human manual driving style. The K-S distance and the K-L divergence are indicators that can measure the similarity between two distributions (Lefèvre *et al.*, 2015b), and are respectively defined as in the following equations:

$$D_{KS}(\mathrm{F}_1||\mathrm{F}_2) = \max_{\mathrm{x}}|F_1(x) - F_2(x)| \tag{14}$$

Table 5. K-S distance and K-L divergence of the proposed planning algorithm and the same driver.

Driver	K-S distance	K-L divergence
1	0.1605	0.1310
2	0.2887	0.2419
3	0.2126	0.2447
Average	0.2206	0.2059

Table 6. K-S distance and K-L divergence of the proposed planning algorithm and the different drivers.

Driver	K-S distance	K-L divergence
1	0.4232 (with driver2)	0.3834 (with driver2)
1	0.2608 (with driver3)	0.4615 (with driver3)
2	0.2828 (with driver1)	0.5197 (with driver1)
2	0.4851 (with driver3)	1.0196 (with driver3)
3	0.2686 (with driver1)	0.1567 (with driver1)
3	0.5788 (with driver2)	0.3159 (with driver2)
Average	0.3832	0.4761

$$D_{KL}(P_1||P_2) = -\sum P_1(x)\log\left(\frac{P_2(x)}{P_1(x)}\right) \tag{15}$$

where, $P_1(x)$ and $P_2(x)$ denote the Probability Density Function (PDF) of x and $F_1(x)$ and $F_2(x)$ denote the Cumulative probability Density Functions (CDF) of x for the two different distributions. The K-S distance can compute the maximum differences in the shape and the location of the PDF, while the K-L divergence can calculate the sum of the differences at each index x of the two PDFs.

The similarity between the driving style of the proposed planning algorithm and human manual driving is measured by the similarity of the THW distributions (Wang *et al.*, 2012; Rosenfeld *et al.*, 2015). For both indicators used to measure the similarity between distributions, a large value signifies a large difference. In other words, a small value means that the two distributions are similar. Both indicators were calculated to verify the similarity between the driving data of the proposed planning algorithm personalized to the individual drivers and the driving data of the same driver, used in the algorithm (Table 5). And indicators were also calculated between the driving data of the proposed planning algorithm and the different drivers' driving data as a control target (Table 6). The results in Tables 5 ~ 6 show that the indices in Table 5 have smaller values than the indices in Table 6. Therefore, the simulation results indicate that the proposed planning algorithm can plan the vehicle speed in a personalized driving style in car-following situations.

6. CONCLUSION

In this paper, a personalized speed planning algorithm in car-following situations using the statistical driver model to reflect individual drivers' driving styles is proposed. The statistical driver model predicts the pedal behavior of the driver through the bagged tree-based model using real driving data. The statistical driver model predicts the THW distribution in the near future through the driver features that cause changes in pedal behavior. The personalized speed planning algorithm was designed through a combination of the statistical driver model and the PCB algorithm. The results of simulation study show that the proposed algorithm generated personalized speed trajectories for individual drivers under the same conditions. In addition, the K-S distance and the K-L divergence values show that the THW distribution of the driving data obtained with the proposed planning algorithm was more similar to the actual driver's THW distribution, compared with those of different drivers.

The main focus of this study was to develop a personalized ADAS to enhance driver comfort in the most frequent driving situation, the car-following situation. The proposed approach has the potential to be applied to other longitudinal driving situations, such as cut-in and cut-out situations. However, to consider various driving situations in which not only the front vehicle but also the surrounding vehicles are involved, it is necessary to integrate radar as well as Lidar and ITS information. With this environment established, as a future work we have a plan to design a personalized ADAS that can reflect individual drivers' driving styles in various driving situations.

ACKNOWLEDGEMENT–This work was financially supported by the Industrial Strategy Technology Development Program (No. 10039673, 0060068, 10079961, 10080284), the International Collaborative Research and Development Program (N0001992) under the Ministry of Trade, Industry and Energy (MOTIE Korea), and National Research Foundation of Korea (NRF) grant funded by the Korean government (MEST) (No. 2011-0017495).

REFERENCES

Angkititrakul, P., Miyajima, C. and Takeda, K. (2011). Modeling and adaptation of stochastic driver-behavior model with application to car following. *IEEE Intelligent Vehicles Symp. (IV)*, Baden-Baden, Baden-Württemberg, Germany.

Bishop, R. (2000). Intelligent vehicle applications worldwide. *IEEE Intelligent Systems and Their Applications* **15**, **1**, 78–81.

Boudali, M., Orjuela, R. and Basset, M. (2020). Unified dynamic and geometrical vehicle guidance strategy to cope with the discontinuous reference trajectory. *Vehicle System Dynamics* **58**, **11**, 1629–1656.

Butakov, V. and Ioannou, P. (2015). Driving autopilot with personalization feature for improved safety and comfort. *IEEE 18th Int. Conf. Intelligent Transportation Systems (ITSC)*, Gran Canaria, Spain.

Caruana, R. and Niculescu-Mizil, A. (2006). An empirical comparison of supervised learning algorithms. *Proc. 23rd Int. Conf. Machine Learning (ICML)*, Pittsburgh, Pennsylvania, USA.

de Gelder, E., Cara, I., Uittenbogaard, J., Kroon, L., van Iersel, S. and Hogema, J. (2016). Towards personalised automated driving: Prediction of preferred ACC behaveour based on manual driving. *IEEE Intelligent Vehicles Symp. (IV)*, Gothenburg, Sweden.

Driggs-Campbell, K., Govindarajan, V. and Bajcsy, R. (2017). Integrating intuitive driver models in autonomous planning for interactive maneuvers. *IEEE Trans. Intelligent Transportation Systems* **18**, **12**, 3461–3472.

Gao, Y. and Gordon, T. (2019). Optimal control of vehicle dynamics for the prevention of road departure on curved roads. *IEEE Trans. Vehicular Technology* **68**, **10**, 9370–9384.

González, D. S., Erkent, O., Romero-Cano, V., Dibangoye, J. and Laugier, C. (2018). Modeling driver behavior from demonstrations in dynamic environments using spatiotemporal lattices. *IEEE Int. Conf. Robotics and Automation (ICRA)*, Brisbane, QLD, Australia.

Gray, A., Gao, Y., Lin, T., Hedrick, J. K. and Borrelli, F. (2013). Stochastic predictive control for semi-autonomous vehicles with an uncertain driver model. *16th Int. IEEE Conf. Intelligent Transportation Systems (ITSC)*, Hague, The Netherlands.

Gu, T., Dolan, J. M. and Lee, J. W. (2016). Human-like planning of swerve maneuvers for autonomous vehicles. *IEEE Intelligent Vehicles Symp. (IV)*, Gothenburg, Sweden.

He, X., Xu, D., Zhao, H., Moze, M., Aioun, F. and Guillemard, F. (2018). A human-like trajectory planning method by learning from naturalistic driving data. *IEEE Intelligent Vehicles Symp. (IV)*, Changshu, China.

Ilić, V., Kukolj, D., Marijan, M. and Teslić, N. (2019). Predicting positions and velocities of surrounding vehicles using deep neural networks. *Zooming Innovation in Consumer Technologies Conf. (ZINC)*, Novi Sad, Serbia.

Joshi, S., Bellet, T., Bodard, V. and Amditis, A. (2009). Perceptions of risk and control: Understanding acceptance of advanced driver assistance systems. *IFIP Conf. Human-Computer Interaction (INTERACT)*, Uppsala, Sweden.

Kale, J. G., Subramaniam, A., Karle, M. L. and Karle, U. S. (2019). Simulation based design and development of test track for adas functions validation and verification with respect to indian scenario. *SAE Paper No*. 2019-26-0100.

Kuwata, Y., Teo, J., Fiore, G., Karaman, S., Frazzoli, E. and How, J. P. (2009). Real-time motion planning with applications to autonomous urban driving. *IEEE Trans. Control Systems Technology* **17**, **5**, 1105–1118.

Lefèvre, S., Carvalho, A. and Borrelli, F. (2015a). Autonomous car following: A learning-based approach.

IEEE Intelligent Vehicles Symp. (IV), Seoul, Korea.

Lefèvre, S., Carvalho, A. and Borrelli, F. (2015b). A learning-based framework for velocity control in autonomous driving. *IEEE Trans. Automation Science and Engineering* **13**, **1**, 32–42.

Lefèvre, S., Carvalho, A., Gao, Y., Tseng, H. E. and Borrelli, F. (2015c). Driver models for personalised driving assistance. *Vehicle System Dynamics* **53**, **12**, 1705–1720.

Li, N., Oyler, D. W., Zhang, M., Yildiz, Y., Kolmanovsky, I. and Girard, A. R. (2017). Game theoretic modeling of driver and vehicle interactions for verification and validation of autonomous vehicle control systems. *IEEE Trans. Control Systems Technology* **26**, **5**, 1782–1797.

Liebner, M., Baumann, M., Klanner, F. and Stiller, C. (2012). Driver intent inference at urban intersections using the intelligent driver model. *IEEE Intelligent Vehicles Symp. (IV)*, Madrid, Spain.

Lin, N., Zong, C., Tomizuka, M., Song, P., Zhang, Z. and Li, G. (2014). An overview on study of identification of driver behavior characteristics for automotive control. *Mathematical Problems in Engineering*, **2014**, 569109.

Lou, Y., Caruana, R. and Gehrke, J. (2012). Intelligible models for classification and regression. *Proc. 18th ACM SIGKDD Int. Conf. Knowledge Discovery and Data Mining*, Beijing, China.

Loulizi, A., Bichiou, Y. and Rakha, H. (2019). Steady-state car-following time gaps: An empirical study using naturalistic driving data. *J. Advanced Transportation*, **2019**, 7659496.

Martinez, C. M., Heucke, M., Wang, F. Y., Gao, B. and Cao, D. (2017). Driving style recognition for intelligent vehicle control and advanced driver assistance: A survey. *IEEE Trans. Intelligent Transportation Systems* **19**, **3**, 666–676.

Mikami, K., Okuda, H., Taguchi, S., Tazaki, Y. and Suzuki, T. (2010). Model predictive assisting control of vehicle following task based on driver model. *IEEE Int. Conf. Control Applications (CCA)*, Yokohama, Japan.

Mitra, P., Choudhury, A., Aparow, V. R., Kulandaivelu, G. and Dauwels, J. (2018). Towards modeling of perception errors in autonomous vehicles. *21st Int. Conf. Intelligent Transportation Systems (ITSC)*, Maui, Hawaii, USA.

Miyajima, C., Nishiwaki, Y., Ozawa, K., Wakita, T., Itou, K., Takeda, K. and Itakura, F. (2007). Driver modeling based on driving behavior and its evaluation in driver identification. *Proc. IEEE* **95**, **2**, 427–437.

Moon, S. and Yi, K. (2008). Human driving data-based design of a vehicle adaptive cruise control algorithm. *Vehicle System Dynamics* **46**, **8**, 661–690.

Ohno, H. (2001). Analysis and modeling of human driving behaviors using adaptive cruise control. *Applied Soft Computing* **1**, **3**, 237–243.

Reagan, I. J., Kidd, D. G. and Cicchino, J. B. (2017). Driver acceptance of adaptive cruise control and active lane keeping in five production vehicles. *Proc. Human Factors and Ergonomics Society Annual Meeting* **61**, **1**, 1949–1953.

Rosenfeld, A., Bareket, Z., Goldman, C. V., LeBlanc, D. J. and Tsimhoni, O. (2015). Learning drivers' behavior to improve adaptive cruise control. *J. Intelligent Transportation Systems* **19**, **1**, 18–31.

Shin, J., Kim, H., Baek, S., Sunwoo, M. and Han, M. (2019). Rule-based alternator control using predicted velocity for energy management strategy. *J. Dynamic Systems, Measurement, and Control* **141**, **12**, 121005.

Wang, J., Zhang, L., Zhang, D. and Li, K. (2012). An adaptive longitudinal driving assistance system based on driver characteristics. *IEEE Trans. Intelligent Transportation Systems* **14**, **1**, 1–12.

Wang, W., Zhao, D., Xi, J., LeBlanc, D. J. and Hedrick, J. K. (2017). Development and evaluation of two learning-based personalized driver models for car-following behaviors. *American Control Conf. (ACC)*, Seattle, Washington, USA.

Wei, J. and Dolan, J. M. (2009). A robust autonomous freeway driving algorithm. *IEEE Intelligent Vehicles Symp. (IV)*, Xi'an, China.

Wei, J., Dolan, J. M. and Litkouhi, B. (2010a). A learning-based autonomous driver: Emulate human driver's intelligence in low-speed car following. *Unattended Ground, Sea, and Air Sensor Technologies and Applications XII*, **7693**, 93–104.

Wei, J., Dolan, J. M. and Litkouhi, B. (2010b). A prediction- and cost function-based algorithm for robust autonomous freeway driving. *IEEE Intelligent Vehicles Symp. (IV)*, La Jolla, California, USA.

Wei, J., Snider, J. M., Gu, T., Dolan, J. M. and Litkouhi, B. (2014). A behavioral planning framework for autonomous driving. *IEEE Intelligent Vehicles Symp. (IV)*, Dearborn, Michigan, USA.

Yang, H. H. and Peng, H. (2010). Development of an errorable car-following driver model. *Vehicle System Dynamics* **48**, **6**, 751–773.

Zhu, B., Jiang, Y., Zhao, J., He, R., Bian, N. and Deng, W. (2019). Typical-driving-style-oriented personalized adaptive cruise control design based on human driving data. *Transportation Research Part C: Emerging Technologies*, **100**, 274–288.